Integrative and Comparative Biology Advance Access published June 9, 2008

Congruence between muscle activity and kinematics in a convergently derived prey-processing behavior

Nicolai Konow,[1] Ariel L. Camp and Christopher P. J. Sanford

Department of Biology, 114 Hofstra University, Hempstead, NY 11549, USA

Synopsis Quantification of anatomical and physiological characteristics of the function of a musculoskeletal system may yield a detailed understanding of how the organizational levels of morphology, biomechanics, kinematics, and muscle activity patterns (MAPs) influence behavioral diversity. Using separate analyses of these organizational levels in representative study taxa, we sought patterns of congruence in how organizational levels drive behavioral modulation in a novel *raking* prey-processing behavior found in teleosts belonging to two evolutionarily distinct lineages. Biomechanically divergent prey (elusive, robust goldfish and sedentary, malleable earthworms) were fed to knifefish, *Chitala ornata* (Osteoglossomorpha) and brook trout, *Salvelinus fontinalis* (Salmoniformes). Electromyography recorded MAPs from the hyoid protractor, jaw adductor, sternohyoideus, epaxialis, and hypaxialis musculature, while sonomicrometry sampled deep basihyal kinesis and contractile length dynamics in the basihyal protractor and retractor muscles. Syntheses of our results with recent analyses of cranial morphology and raking kinematics showed that raking in *Salvelinus* relies on an elongated cranial out lever, extensive cranial elevation and a curved cleithrobranchial ligament (CBL), and that both raking MAPs and kinematics remain entirely unmodulated—a highly unusual trait, particularly among feeding generalists. *Chitala* had a shorter CBL and a raking power stroke involving increased retraction of the elongated pectoral girdle during raking on goldfish. The raking MAP was also modulated in *Chitala*, involving an extensive overlap between muscle activity of the preparatory and power stroke phases, driven by shifts in hypaxial timing and recruitment of the hyoid protractor muscle. Sonomicrometry revealed that the protractor hyoideus muscle stored energy from retraction of the pectoral girdle for ca. 5–20 ms after onset of the power stroke and then hyper-extended. This mechanism of elastic recoil in *Chitala*, which amplifies retraction of the basihyal during raking on goldfish without a significant increase in recruitment of the hypaxialis, suggests a unique mechanism of modulation based on performance-enhancing changes in the design and function of the musculoskeletal system.

Introduction

Modulated behavioral responses, or the ability of an organism to perform a consistent behavioral change elicited by differences in biophysical stimuli, may allow an organism to optimize its performance efficiency (Wainwright and Lauder 1986; Nemeth 1997a; Ralston and Wainwright 1997; Ferry-Graham 1998; Ferry-Graham et al. 2001; Bolnick and Ferry-Graham 2002). Thereby, the organism may channel and increase its versatility (Roth and Wake 1985; Galis 1993; Nemeth 1997b) and ultimately broaden its range of utilization of resources (Liem 1979; Ralston and Wainwright 1997). Increases in fitness resulting from behavioral modulation may both promote ecological success and ultimately drive phylogenetic diversification (Streelman and Danley 2003). Prompted by Liem's (1978, 1979) work on cichlid feeding, which resulted in a theorem predicting that trophic generalists are more likely to gain fitness from behavioral modulation than are trophic specialists, the concept of behavioral modulation has been extensively studied. The structural and functional aspects of this concept are now well understood at discrete organizational levels of feeding behaviors in basal aquatic vertebrates, including the output kinematics (Wainwright and Lauder 1986; Nemeth 1997a, 1997b; Ferry-Graham 1998; Wilga and Motta 1998; Ferry-Graham et al. 2001) and the underlying muscle activity patterns (MAPs) (Wainwright 1986; Deban et al. 2001; Korff and Wainwright 2004).

Analyses evaluating congruence among organizational levels of musculoskeletal function (Lauder and Reilly 1996) are considered a powerful tool in understanding the evolution of diversity, but remain uncommon, and mostly focused on the capture of prey (Aerts and De Vree 1993; Lauder and Reilly 1996; Wilga and Motta 1998; Motta and

From the symposium "Electromyography: Interpretation and Limitations in Functional Analyses of Musculoskeletal Systems" presented at the annual meeting of the Society for Integrative and Comparative Biology, January 2–6, 2008, at San Antonio, Texas.

[1]E-mail: nicolai.konow@hofstra.edu

Integrative and Comparative Biology, pp. 1–15
doi:10.1093/icb/icn045

Wilga 2001). An important pattern emanating from these studies is that modulation responses segregate into those elicited by differences in size of prey (prey-size hypothesis: Anderson 1993; Nemeth 1997a, 1997b; Ferry-Graham 1998; Motta and Wilga 2001; Ajemian and Sanford 2007) or contrasting biomechanical challenges, such as elusiveness of prey, sturdiness of attachment (Lauder and Prendergast 1992; Ferry-Graham et al. 2001; Van Wassenbergh et al. 2006), and malleability of prey (Wainwright and Lauder 1986; Ralston and Wainwright 1997; Sanford 2001b). To further explore this segregation, we used a multi-level analysis to comprehensively quantify modulation in a different functional system, the tongue-bite apparatus (TBA). This novel jaw apparatus governs a convergently derived raking prey-processing behavior, which is used by osteoglossomorphs and salmonids, two major and historically unrelated lineages of bony fish, to immobilize and reduce prey. (Sanford 2000, 2001a, 2001b; Konow and Sanford 2008).

Modulation elicited by biomechanical differences between prey types was previously quantified in the raking kinematics of *Chitala ornata* (knifefish), an osteoglossomorph trophic specialist (Rahman 1989; Lim et al. 1999). Rakes on robust, elusive fish prey (see Supplemental Material online) resulted in an increased magnitude and velocity of retraction of the pectoral girdle relative to that occurring when processing sedentary, malleable worm prey (see Supplemental Material online) (Frost and Sanford 1999). Neurocranial elevation, described by a third-order lever system (Carroll 2004), commenced earlier during processing of robust prey and augmented motion of the pectoral girdle, which was primarily responsible for driving the raking power stroke (Frost and Sanford 1999). In contrast, the brook trout, *Salvelinus fontinalis*—a salmonid trophic generalist—used unmodulated raking kinematics on three biomechanically contrasting types of prey (goldfish [see Supplemental Material online], worm [see Supplemental Material online], and cricket). Raking in *Salvelinus* involved a magnitude of neurocranial elevation only surpassed in *Xenomystus*, a close relative to *Chitala* (Sanford 2001a) and was augmented by retraction of the pectoral girdle (Sanford 2001b).

In a parallel analysis of TBA morphology in *Salvelinus* and *Chitala*, we have established quantitative differences in myology and osteology that offer at least partial explanations of the observed interspecific differences in ability or propensity to modulate. *Salvelinus* has a longer cranial out-lever distance, a longer supracleithrum, and a larger anatomical cross-sectional area of the epaxialis (EP), hypaxialis (HP), and hyoid protractor muscle, whereas *Chitala* has a larger sternohyoideus (SH) muscle. The cleithrobranchial ligament (CBL) is arc-shaped in salmonids, in contrast with the straight morphology of this ligament in osteoglossomorphs. Such qualitative anatomical differences may have drastic functional consequences on raking and other feeding behaviors (Hilton 2001), and by extension, this could apply to TBA-bearing teleosts in general (Konow and Sanford 2008). The CBL may duplicate the SH, which often has a labile feeding MAP (Sanford and Lauder 1989; Carroll 2004). Differences in CBL shape are thus likely to influence the ability of this ligament to transfer strain generated by the HP via the pectoral girdle to the hyoid. This would affect the extent to which the SH may be functionally decoupled and allowed to act as a modulator muscle during the raking power stroke.

The study taxa examined here and in the parallel morphological study are representatives of two lineages known to use raking behaviors, and both taxa have a basihyal adorned with hypertrophied and posteriorly-curved fang-like dentition that may shear the prey during the raking power stroke (Lauder and Liem 1980; Sanford and Lauder 1989; Sanford 2001b; Hilton 2003). However, basihyal kinematics during raking and an alternative prey processing behavior, open-mouth chewing, remain unquantified. The predicted posterior direction of the basihyal during raking represents a marked deviation from the typical depression pattern of the anterior hyoid during fish strikes (Sanford and Wainwright 2002). A posterior-directed basihyal movement would also explain the considerable prey reduction observed when raking taxa occasionally eject prey (Konow and Sanford, personal observation). This would be a result of the fang-toothed basihyal shearing the prey while it is impaled on the dorsal TBA dentition and anchored by the oral jaws (Sanford and Lauder 1989; Frost and Sanford 1999; Sanford 2001a, 2001b). Still, the hypothesis that basihyal trajectories in these taxa should converge does conflict with the clear differences in input that the neurocranium and pectoral girdle contributes to the kinematics of the raking power stroke in *Chitala* and *Salvelinus* (Frost and Sanford 1999; Sanford 2001b). Alternatively, convergent basihyal trajectories during raking could result from differences in the pattern of modulation in muscle activity. Therefore, these taxa are particularly interesting for testing hypotheses about musculoskeletal function and the role of behavioral modulation in the convergently derived TBA.

We used sonomicrometry recordings of basihyal kinesis and length dynamics in the basihyal protractor and retractor musculature during raking, synchronized with high-speed video of external kinematics to make our data directly comparable with existing evidence. Synchronized EMG was recorded from muscles that are known to be important in raking (Sanford and Lauder 1989; Konow and Sanford 2008). By synthesizing these results with previously published kinematics data (Frost and Sanford 1999; Sanford 2001b) and unpublished TBA morphology (A. Camp, N. Konow and C. Sanford, unpublished data) for these taxa, we could focus on relationships existing between the organizational levels responsible for modulation of raking. Modulation is defined as a statistically different kinematic or muscle activity pattern in response to different stimuli (see also Nemeth 1997a, 1997b; Frost and Sanford 1999).

The aim of this study was a comprehensive quantification of raking in order to determine if: (1) the power-stroke kinematics of the basihyal diverge between *Chitala* and *Salvelinus*, and (2) if shifts in MAP activity (onset and offset timing) or recruitment (mean amplitude and integrated area) explain previously observed kinematic changes, or if such muscle activity-shifts are absent and the observed changes primarily are attributable to interspecific differences in morphology. The priority on obtaining MAP data is underscored by the lack of modulation of raking kinematics in *Salvelinus* (Sanford 2001b). The absence of modulation in a trophic generalist such as *Salvelinus* is in stark contrast to Liem's theorem (1978, 1979), and a lack of MAP modulation has never been reported in feeding studies (Wainwright and Friel 2000, 2001).

We tested three specific hypotheses: (1) Although no modulation occurs in the raking kinematics of *Salvelinus* (Sanford 2001b), raking MAP modulation should occur, according to Liem's (1978, 1979) principle that trophic generalists should modulate. (2) Modulated responses in the kinematics of raking in *Chital*a (Frost and Sanford 1999) should be congruent with modulation of raking MAPs, specifically involving modulation of the recruitment of both the HP and SH. (3) Trajectories of the basihyal during raking power strokes in the study taxa (a) should differ from chewing motions and (b) should diverge between taxa, given the previously established differences in the kinematics of raking in these taxa (Sanford and Lauder 1989; Frost and Sanford 1999; Sanford 2001b).

Materials and methods

Specimens and husbandry

All specimens of brook trout [*Salvelinus fontinalis* (Mitchill)] were obtained from the Cold Spring Harbor fish hatchery, Long Island, New York, and knifefish [*Chitala ornata* (Gray)] of similar size were purchased from Long Island Aquatics, NY. The anatomy of the TBA and electromyography (EMG) of raking were investigated in different samples of study animals. The specimens used for kinematic analyses (Frost and Sanford 1999; Sanford 2001b) did not differ significantly in size from those used for morphological analyses [*t*-test; *Salvelinus* ($N=4$), $P=0.39$; *Chitala* ($N=4$), $P=0.34$]. For EMG, similar sized *Salvelinus* ($N=5$, head lengths, HL = 57–69 mm; mean = 63 mm ± 0.79 SEM) and *Chitala* ($N=5$, HL = 62–77 mm; mean = 65 mm ± 0.81 SEM) were used. Head lengths did not differ significantly among EMG individuals (paired *t*-test, $t_4=0.794$; $P=0.472$), which is important since body size may influence both kinematic and EMG variables (Wainwright and Richard 1995). All specimens were housed individually in aquaria at the Hofstra University animal care facility, according to applicable ethics and animal care (IACUC) approvals. *Salvelinus* were kept at ca. 15°C and *Chitala* at ca. 27°C as per Ojanguren and Brana (2000) and Sanford (2001a, 2001b). During acclimation, which often lasted a month, a mixed diet of goldfish (*Carassius*), earthworms (*Lumbricus*), crickets (*Gryllus*), and minnows (*Pimephales*) was fed to the animals under floodlight illumination to avoid habituation to one type of prey during routine provisioning and to accustom them to feeding when illuminated. Experiments were only commenced on animals that fed aggressively and appeared well acclimated. Levels of motivation were standardized among individuals and experiments by depriving them of food for two days prior to an experiment.

Electromyography

To focus on the level of stereotypy in MAPs we used five replicates to obtain a more accurate quantification of intraspecific variability in motor-patterns (Wainwright et al. 1989). EMGs were recorded from five muscles that are commonly involved in vertebrate aquatic feeding (Wainwright et al. 1989; Grubich 2001) and have been argued to be important during raking (Sanford and Lauder 1989; Sanford 2001a, 2001b; Konow and Sanford 2008): the protractor hyoideus (PH) in *Salvelinus* [homologous with the posterior intermandibularis (PIM) in *Chitala*; see Sanford and Lauder 1989], sternohyoideus (SH), adductor mandibularis (AM), epaxialis (EP), and hypaxialis (HP) muscles (Fig. 1). We used a modified EMG protocol from previous studies (Wainwright et al. 1989; Alfaro and Westneat 1999; Konow and Sanford 2008): fine-wire bipolar

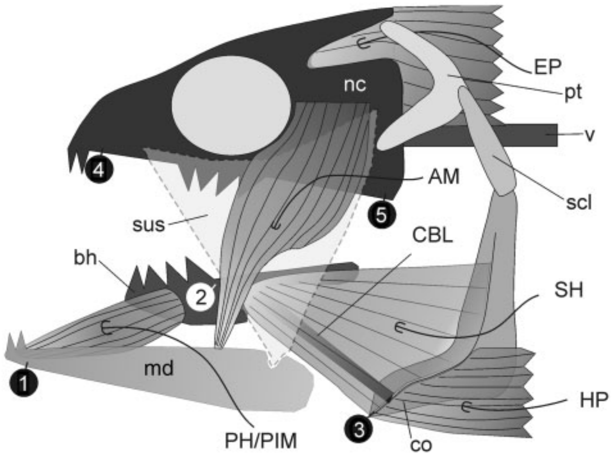

Fig. 1 Diagram of a TBA, with the five muscles sampled using EMG (curved arrows): PH/PIM, protractor hyoideus in *Salvelinus*, functionally homologous to the PIM in *Chitala* (Lauder and Sanford 1989). The CBL is medial to the sternohyoideus (SH) muscle, which is medial to the suspensorium (SUS); the AM is the most superficial; EP, epaxialis; HP, hypaxialis. Sonomicrometric crystals were sutured to the: 1, mandibular (md) angle; 2, basihyal (bh) keel; 3, coracoid (co) keel; 4, anterior neurocranium; and 5, posterior neurocranium (nc) to quantify deep cranial kinesis. Other bones: pt, post-temporal; scl, supracleithrum; v, vertebral column.

hook-electrodes were prepared by threading 1.25 m lengths of double-stranded wire (0.05 mm diameter polyethylene-coated stainless steel; California Fine Wire, CA) through 25 5/8 gauge hypodermic needles. Hooked electrode ends with 0.5 mm exposed tips and bipolar spacing was fashioned under a microscope using watchmaker's forceps. Electrodes were implanted under the trailing edge of a scale at a 45° angle to the surface of the muscles on the left side of animals anaesthetized using 40 p.p.m. alcoholic Eugenol (Munday and Wilson 1997).

During implantation, the electrode hooks were anchored percutaneously into the muscle bellies parallel to the orientation of muscle fibers (Fig. 1). Electrode wires were then anchored to a mid-dorsal suture on the specimen and joined with glue while the ends of the electrode connectors were crimped into din-25 adapter pins. Floats were taped to the electrode wires to prevent the specimen from tangling with these during the experiment. Rather than verifying the placement of electrodes by dissection after each experiment, we used repeated practice implants on sacrificed and unpreserved conspecifics, followed by dissections to verify fiber orientation and electrode placement. Accuracy of implantation was optimized even further by the large size of the study animals and their muscles as well as the easy identification of target muscles, given their superficial placement, and clear delineation from other muscles.

During experiments, prey consisting of elusive and robust live goldfish (30–40 mm TL) approximating the lateromedial gape width of the study animal and similar-sized sedentary and malleable Canadian night crawlers (*Lumbricus* sp.) were released at random to the study animal. The study animal typically caught the prey in a rapid ram-suction strike and proceeded with prey-processing using both raking and open-mouth chewing behaviors. It was beyond the scope of this project to investigate the role of variability in the activity of individual muscles across different behaviors for a single type of prey (for such an analysis, see Konow and Sanford 2008). Instead, we aimed to determine the effect of type of prey on the variability in muscle activity. EMGs of muscle activity during capture and processing of prey were sampled at 10 kHz, amplified 1000 times (A-M systems, differential AC amplifier, model 1700, Everett, WA, USA), and conditioned with a 100–1000 Hz band-pass and a 60 Hz notch filter engaged. EMG signals, sonomicrometric distances (see below) and a manual trigger-code (+5 V) used to label the behaviors during recording were digitized via a PowerLab 16/30 system using Chart v.5.5.5 for Windows (ADInstruments, Colorado Springs, CO).

Extraction of EMG data

After each experiment, sections containing noise from manipulation of the electrode wires were removed from the EMG trace and the remaining behavioral signals were logged according to type of behavior (indicated by the trigger-code), type and size of prey, orientation of prey in the mouth of the predator during prey-processing and the orientation and motivation exhibited by the predator, all using the comments tool in Chart. This information guided subsequent selections of EMGs for analysis. Although we observed the predators feeding aggressively on several prey items before displaying satiation, for analysis we only selected EMGs from the first three feedings of each experiment. These always involved aggressive processing of prey that was placed head or tail first in the oral cavity of the predator.

From the rectified EMG signals of each muscle (Fig. 2), we measured 20 muscle activity variables, divided into five groups (Fig. 3): (1) duration of muscle activity (from first to last activity burst in the sampled muscle, measured in ms); (2) MAP onset (ms), relative to onset time of activity in the EP muscle (reference muscle); (3) mean amplitude

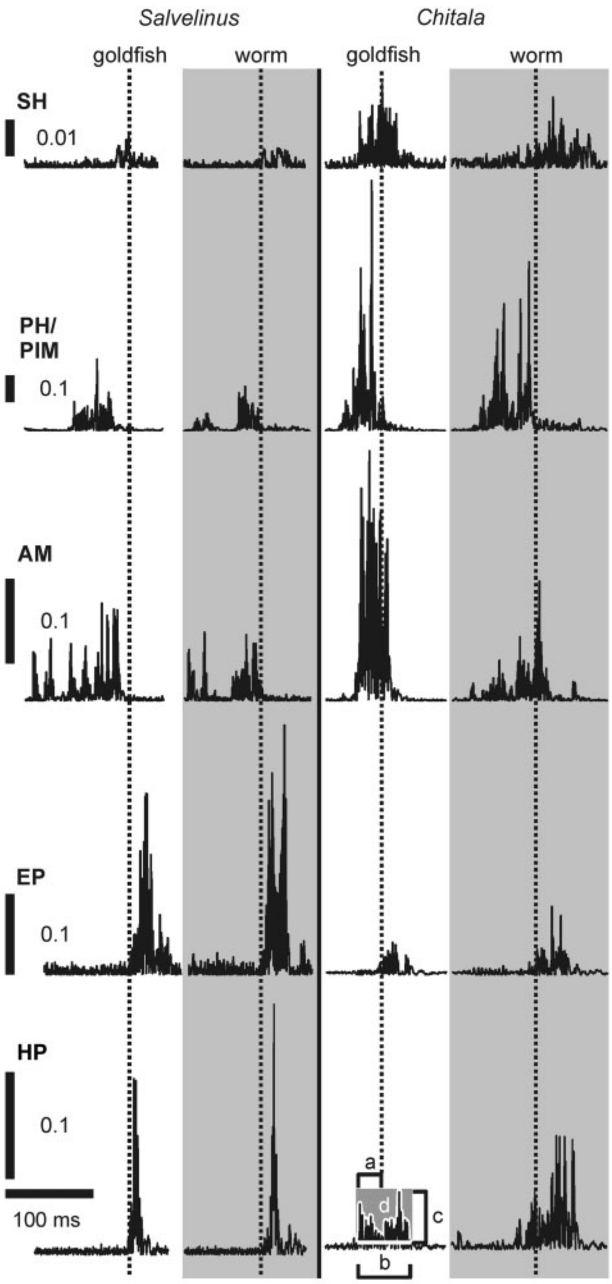

Fig. 2 Rectified EMGs representing typical raw data from raking behaviors in *Salvelinus* (left) and *Chitala* (right). Data for the five sampled muscles are shown: SH, sternohyoideus; PH, protractor hyoideus (*Salvelinus*); PIM, posterior intermandibularis (*Chitala*); AM, adductor mandibularis; EP, epaxialis; HP, hypaxialis. Measured variables are indicated by: [a] onset time of activity relative to onset time of EP activity (vertical dashed lines) and [b] duration of activity (ms); [c] mean spike-scaled amplitude (mV-ratio); [d] integrated area (mV × s), an intensity measurement of the signal-area under the rectified EMG signal, and over the signal baseline (delineated by the signal component outlined by white inside the grey box).

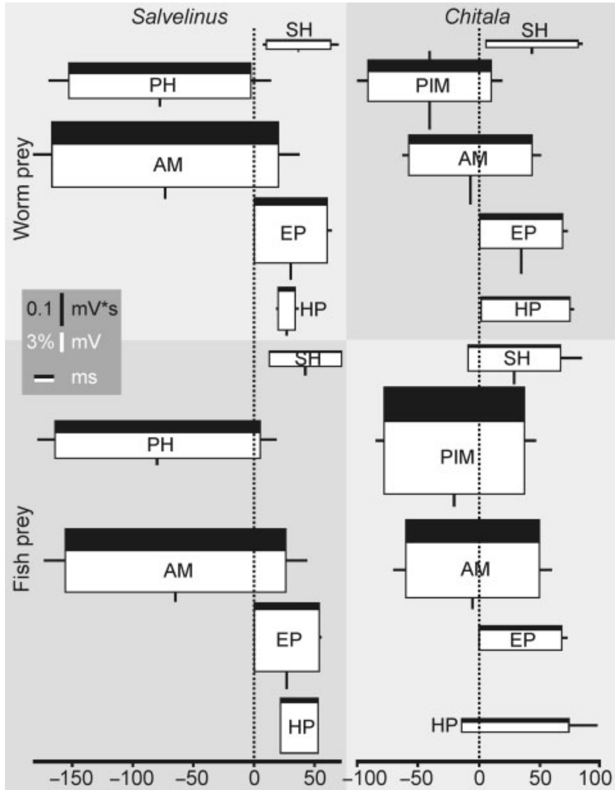

Fig. 3 Composite EMG bar plots of activity (*x*-axis; in ms) and recruitment variables (*y*-axis) for raking on worms and fish by *Salvelinus* and *Chitala*. Boxes depict mean values for each muscle. (See also online table as supplemental material). For abbreviations, see Fig. 1. *X*-axis shows onset-time (left box margin) relative to EP onset (vertical dashed line) which delineates onset of the raking power stroke, and activity offset (right box margin). Height of upper dark box is mean integrated area (mV × s) and height of the bottom light box represents mean amplitude, both variables scaled as a percentage of maximum spike-amplitude. Whiskers are SEM. Note that early SH and HP activity, and prolonged PIM and AM activity, characterizes raking on goldfish by *Chitala*.

Table 1 Summary statistics for DFA of activity of muscles used in raking run separately for *Salvelinus* and *Chitala*

Mahalanobis distance	*Salvelinus*		*Chitala*	
	Axis 1	Axis 2	Axis 1	Axis 2
Prey-type effect ANOVA	$F_{2,32} = 6.22$	$F_{2,32} = 8.84$	$F_{2,38} = 23.47$	$F_{2,38} = 88.47$
Hypothesis testing	$P = 0.213$	$P = 0.053$	$P < 0.001$**	$P < 0.001$**

**Significant after Bonferroni correction.

(signal intensity) in mV, scaled as a percentage of the maximum amplitude (spike) recorded from the muscle in question during a specific experiment (implant-correction), whilst sampling across all prey and recorded behaviors (strike, rakes, and chews); and (4), integrated area (signal energy), i.e., "area under the curve", but above the signal baseline, in mV × s, scaled as a percentage of the same maximum amplitude spike. Total rake duration (5), the time from onset of the first muscle activity to the offset of the last (in ms) during each rake was calculated for comparison, but not used in the statistical analyses.

For activity variables, the time during which amplitude of the signal exceeded three-fold or greater than the baseline was used as a cutoff. To ascertain whether further recruitment variable corrections were necessary, we generated data subsets containing recruitment variables (amplitude and integrated area) with all spikes included and with spikes removed at the 50% amplitude level, and with or without the use of signal-binning at 10 ms time-intervals. Correlation analyses verified that the spike-free and binned data were statistically similar to the original data, with all variables being significantly correlated (Pearson correlation range; 0.67–0.98; minimum $P = 0.12$). Thus, we omitted spike-removal and binning and analyzed the original data subsequently. Parametric analyses (see below) were also performed on separate datasets of scaled and non-scaled recruitment variables, and integrated area was the only variable type where correction of peak-amplitude did not alter the resulting PC-factor scores and component loadings (visually assessed in plots). Therefore, to retain potentially important biological information in the dataset, our final statistical analyses examined EMG values of scaled amplitude and of non-scaled integrated area.

Sonomicrometry and high-speed video

Lateral and ventral high-speed video only provides cursory evidence, at best, of movement of the basihyal during feeding, as it is often obscured by more lateral bony elements. We therefore used synchronized sonomicrometry and high-speed video on three specimens from each taxon, using a modified protocol from Sanford and Wainwright (2002). During implantation of EMG electrodes, the mandibular symphysis, the anterior and posterior roof of the mouth, and the ventral keels of the basihyal and coracoid were palpated to identify suitable positions where 2-mm piezoelectric crystals (Sonometrics Corp., London, ON, Canada) could be attached to the integument with sutures (Fig. 1). Suturing crystals to the integument rather than implanting them into muscles provides an accurate measure of musculoskeletal kinesis while minimizing invasive surgery (Konow and Sanford 2008). Repetitive expansive and compressive manipulations of the head of the anesthetized fish were used to verify the sturdiness and to estimate movement of crystals at their attachment (ca. 2 mm). The distance between crystal [4] and [5], which remained unaltered by cranial kinesis in the feeding fish, was measured as a reference using calipers. During experiments, we recorded changes in distance between the basihyal [2] and the anterior [4] and posterior [5] roof of the mouth. Length-dynamics in the basihyal protractor (PIM/PH) and retractor (SH) muscles were measured by proxy of changes in the distance from the basihyal [2] to the mandibular symphysis [1] and to the coracoid keel [3]. While surgery involving both EMG and sonomicrometry instrumentation lasted ca. 60 min, all fish recovered ca. 20 min after surgery.

Sonomicrometry data were recorded at a sample rate of 500 Hz and a transmit pulse of 220 ns with an inhibit delay of 1.7–2.2 mm and inspected in SonoView (Sonometrics Corp., London, ON, Canada). For the purpose of data-synchronization, analog sonometric signals were recorded at 10 kHz on four channels of the EMG PowerLab system (distance 4–5 was constant, ±0.5mm). Data on distances between pairs of crystals were exported as ASCI files from SonoView to Microsoft Excel and raking basihyal movement loops (Sanford and Wainwright 2002) and muscle length-dynamics (Konow and Sanford 2008) were plotted.

Conventional motion-analyses of high-speed videos, recorded in synchrony with EMG, and sonomicrometric data were used to quantify elevation of the neurocranium and kinematics of the pectoral girdle. Onset time of neurocranial elevation was used as $\boldsymbol{t}_0$ to align basihyal motion loops (see later) in order to obtain 95% confidence intervals for basihyal kinesis and to align plots of muscle length dynamics. Linear regressions were used to relate maximum displacement of the basihyal to maximum displacement of the pectoral girdle and to length dynamics in the basihyal protractor and retractor musculature. Performance-plots were used to illustrate the relationship of pectoral girdle retraction with length dynamics in the basihyal protractor and retractor musculature.

Statistical design

Means and standard errors for all derived variables were calculated (See comment in Fig. 3 legend.) and summarized in bar plots for species-specific raking behaviors (Fig. 3). Discriminant function analysis (DFA) with MANOVA was used to partition variance, and the accuracy of species-prey group predictions was evaluated using jack-knifed classification matrices. Variables were accepted as significant explanations of variance when canonical discriminant functions (CDF), standardized by within-variance, were $> \pm 0.6$. Mahalanobis (MH) distances obtained from the DFA were arranged along separate axes, analogous to a principal component analysis recovering axes of PC factor-scores (Fig. 4). To isolate the effect of prey-type from the effect of individual variability, we used two-way mixed-model ANOVAs separately on each MH distance axis, with prey-type as fixed-effect and individual as random-effect (Reilly and Lauder 1989). Subsequent tests of hypotheses used the Mean Square of the interaction term between the fixed and the random effects (prey/individual) as the denominator for the main effect (prey), following Zar (1999). The analyses above were conducted separately for each species since a direct comparison of species was beyond the scope of this study (See Konow and Sanford 2008 for such analyses). However, canonical correspondence axis-pairs for each taxon were plotted together (Fig. 5) to illustrate the segregation of raking behaviors specific to prey type across available regions of multivariate space for muscle activity (Fig. 5A) and kinematics (Fig. 5B).

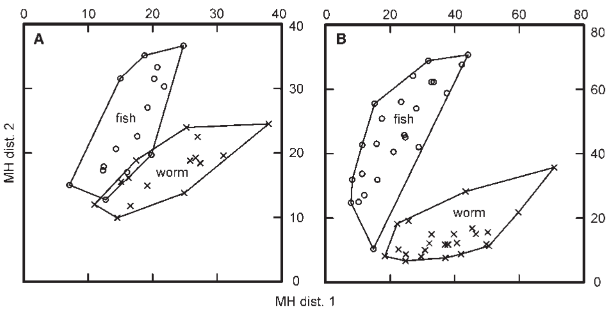

Fig. 4 Bi-plots of MH distance-axes 1 and 2 from DFA of 19 variables of muscle activity in (**A**) *Salvelinus* and (**B**) *Chitala* raking on fish and worms. Note that prey-type specific MH distances overlap slightly in *Salvelinus* and segregate completely in *Chitala*.

Results

Muscle Activity of the Tongue-Bite Apparatus

A qualitative investigation of MAPs revealed both timing and recruitment differences between the two taxa, although differences between the two types of prey only were discovered in *Chitala*. Mean MAPs for *Salvelinus* (Fig. 3) are very similar between types of prey, although activity of the HP appears prolonged during raking on goldfish. Recruitment (meaning the variables mean amplitude and integrated area) of the EP is greater in *Salvelinus* than *Chitala* (below) for both prey-types. Both recruitment variables for the SH muscle have an order of magnitude lower intensity during raking on worm prey than other muscles quantified in this study and were more intense but also relatively variable during raking on goldfish in both taxa. In *Chitala*, the preparatory phase starts significantly earlier during rakes on both prey types, and activity in the AM, PIM, and HP lasts longer than in *Salvelinus*. During goldfish rakes, the SH amplitude increases while EP and HP amplitudes decrease and activity of the HP is extended well into the power stroke compared to worm rakes.

Separate DFAs were run on the EMG datasets from *Salvelinus* and *Chitala* to determine if there was

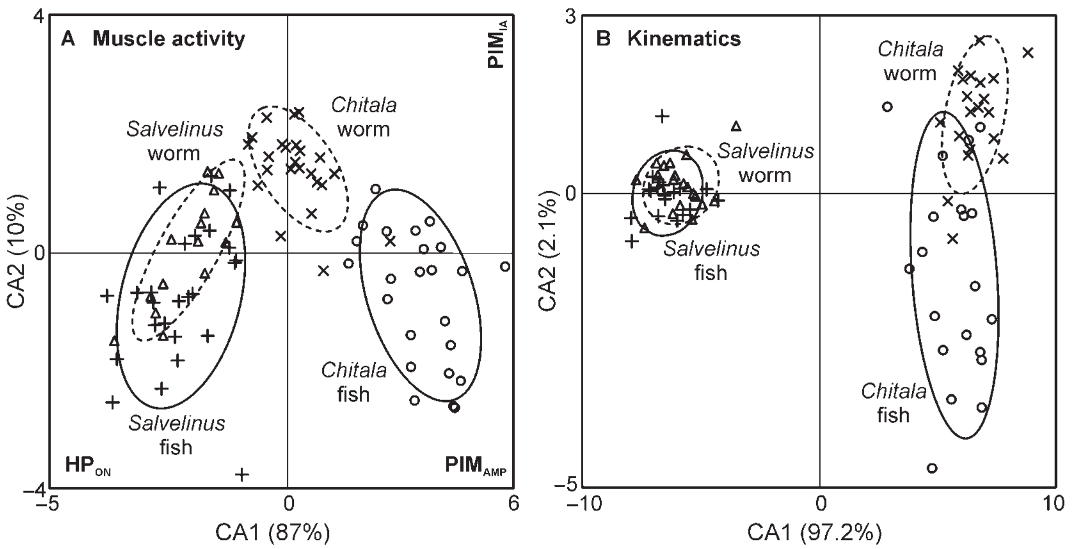

Fig. 5 Biplot of significant canonical correspondence axes from DFA of (**A**) muscle activity from *Salvelinus* and *Chitala* raking on fish and worms (this study) and (**B**) corresponding data on the kinematics of raking (from Frost and Sanford 1999; Sanford 2001). The primary axes (CA1) explain overriding proportions of variance in both datasets. *Salvelinus* shows almost complete prey specific overlap in both datasets. Meanwhile, prey specific data from *Chitala* segregate completely across MAP space, while overlapping partially across kinematic space. Variable labeling in (A) is explained in caption of Table 2.

Table 2 Canonical Discriminant Functions (CDF) from a DFA on activity of raking muscles in both study taxa

Variable	CCA1	CCA2	ANOVA[a]
SH duration	0.267	0.438	ns
SH onset	−0.238	**0.718**	ns
SH amplitude	0.278	−0.331	ns
SH area	0.382	−0.070	ns
Hyoid protractor duration	**1.156**	**−2.330**	ns
Hyoid protractor onset	**1.649**	**−1.590**	ns
Hyoid protractor amplitude	0.705	−1.282	**
Hyoid protractor integrated area	0.040	**1.043**	**
AM duration	**1.076**	−0.550	ns
AM onset	**1.187**	−0.498	ns
AM amplitude	0.293	−0.227	*
AM integrated area	0.087	−0.180	**
EP duration	−0.208	0.090	ns
EP amplitude	−0.593	−0.232	ns
EP area	0.255	−0.110	ns
HP duration	−0.115	0.369	ns
HP onset	**−0.775**	0.151	*
HP amplitude	−0.413	−0.122	***
HP integrated area	−0.140	−0.492	ns

[a]Prey-type effect ANOVAs on *Chitala* muscle activity raw data. Significant after Bonferroni-correction; $*P = 0.05$; $**P < 0.01$; $***P < 0.001$.
Canonical correspondence Axes (CCA) 1 and 2 each described over 10% each of the variance in the dataset (Fig. 5 A). Variables (boldface) loading strongly in the DFA (CDF > 0.6; boldfaced), and differing significantly between both types of prey for *Chitala* (Bonferroni corrected ANOVA on raw data on muscle activity, $P < 0.05$; right column) were deemed behaviorally modulated (see also Fig. 5 A). For variable explanation, please see text.

a prey-type effect at the level of MAP. The DFA on *Salvelinus* accounted for 79.5% of variance present in the dataset and returned two MH distance axes (Fig. 4A). MANOVAs on the MH distance scores did initially recover significant differences in muscle activity between prey types (Wilk's $\lambda = 0.335$; $F_{2,23} = 22.81$; $P < 0.001$). However, accuracy of classification by type of prey was low (40% for rakes on goldfish and 53% for rakes on worm) which indicated an overriding role of individual behavioral variability, and the initial prey-type effect did not withstand Bonferroni-corrected *post hoc* tests. The DFA on the MAP data from *Chitala* (Table 1) accounted for 92% of the variance in the dataset and also returned two MH distance axes. A MANOVA on these MH distances recovered significant MAP differences between prey types (Wilk's $\lambda = 0.105$; $F_{2,38} = 162.304$; $P < 0.001$). Accuracy of classification by type of prey was high (79% of rakes on goldfish and 96% of rakes on worms), and both MH distance axes (Fig. 4B) remained significant for prey type after *post hoc* tests ($P < 0.001$; Table 1).

With the presence of a prey-type effect in *Chitala* established, we ran a DFA on the combined EMG datasets for both taxa (Fig. 5A) in order to assess which MAP variables were responsible for dispersing prey-specific raking behaviors in *Chitala* across multivariate space. Eleven of the 19 CDF loaded strongly along the significant canonical correspondence axes (CDF>0.6; Table 2). To identify which variables that differed significantly between rakes on worm and goldfish prey in *Chitala*, we used Bonferroni-corrected ANOVAs on the raw EMG data for this taxon alone. Only variables with a significant ANOVA on the raw EMG data for *Chitala*, and a CDF>0.6 on the combined MAP datasets for both taxa were deemed statistically different between prey-types in *Chitala*. In this way, variables with a prey-type effect in *Chitala* were confidently distinguished from those that either drove interspecific differences or statistically non-significant differences between prey-types in *Salvelinus* (the latter having CDFs >0.6, but ns ANOVA results for *Chitala* in Table 2). Three MAP variables showed significant prey-type differences in *Chitala* (Table 2), reflecting earlier activity in the HP and amplified recruitment variables for the PIM during goldfish raking (Fig. 3).

A DFA on the combined kinematic datasets for the study-taxa, originating from Frost and Sanford (1999) and Sanford (2001b) were used to compare behavioral-relative to taxon segregation across the organizational levels of muscle activity and kinematics. Whilst the plots for each level (Fig. 5) are similar, important differences are apparent: in both analyses, Canonical Axis 1 (CA1) explains an overriding amount of dataset variance (87–97%), while the dispersal of taxa and prey-type specific cases for *Chitala* is more pronounced along CA1 of multivariate MAP space. *Salvelinus*, on the other hand, shows highly stereotypical raking kinematics, and a slightly more variable MAP of raking (cf. Fig. 5A against Fig. 5B), as also indicated by the ANOVA for *Salvelinus* MAP, which approached significance along MH distance 2 ($P = 0.053$; Table 1).

Basihyal movements and muscle contraction

Sonomicrometry revealed that despite clear interspecific differences in the external kinematics of raking (see online video files of raking in the two taxa and Fig. 5B) raking basihyal movements in *Salvelinus* and *Chitala* have very similar trajectories. Clear distinctions also exist between basihyal movements during the raking preparatory, power stroke,

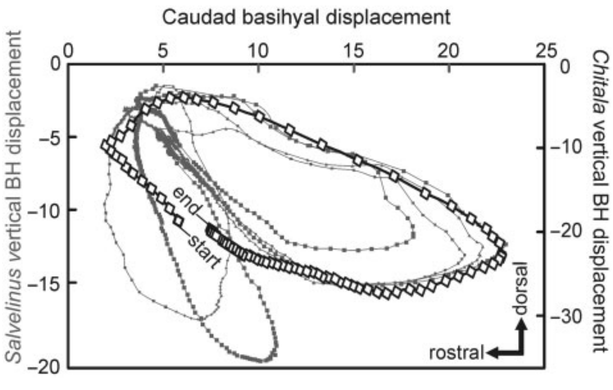

Fig. 6 Representative basihyal motion loops for processing of goldfish prey measured using sonomicrometry in two size-matched specimens of *Salvelinus* and *Chitala*. Both axes are in mm. The origin (0,0) corresponds with location of the anterior crystal ([4] in Fig. 1), while the posterior crystal [5] was placed ca. 25 mm caudally. For *Salvelinus* (grey line; filled symbols), four rakes (horizontal loops) are interspersed by two chews (vertical loops). An almost completely convergent basihyal trajectory during the raking power stroke is seen in *Chitala* (black line; open symbols). In both taxa, basihyal excursion velocities are higher during power strokes than during recovery and preparatory phases, as indicated by an increase in distance between markers (500 Hz sampling) in the upper right portion of the graphs. Experimental and analytical methods follow Sanford and Wainwright (2002).

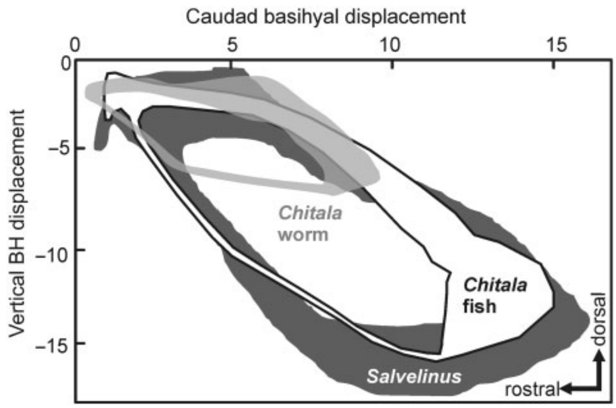

Fig. 7 Quantitative basihyal movement loops (ellipse margins delineate 95% confidence intervals) in *Salvelinus* in which no effect of prey type was found, and in *Chitala*, in which the basihyal during raking of worms is retracted ~40% compared to raking on goldfish. Plot orientation and scaling as in Fig. 6.

and recovery phases (Fig. 6). In both taxa, the basihyal is protracted slowly during the *preparatory phase* and elevated towards the prey in the anterior oral cavity, coincident with adductor mandibulae contraction closing the oral jaws. During the subsequent raking *power stroke*, basihyal kinesis is more rapid (nearly 20 cm/s) and posterior directed, at the end altering towards a posteroventral trajectory, while slow basihyal protraction occurs during the *recovery phase*. In contrast, open-mouth chewing (Sanford and Lauder 1989; Konow and Sanford 2008) involves a distinctly different, dorsoventrally directed basihyal trajectory (Fig. 6). Basihyal movement loops were aligned for each taxon- and prey-specific category at the onset time for neurocranial elevation (t_0), so that 95% confidence ellipses could be obtained. These ellipses showed that basihyal trajectories during raking in *Salvelinus* remained unaltered by different prey types, while *Chitala* did show a prey-type effect (Fig. 7). While the ellipses overlap for *Salvelinus* rakes and *Chitala* rakes on goldfish prey, indicating highly similar raking kinematic outputs, a significantly reduced basihyal excursion during *Chitala* raking power strokes on worm prey is also apparent.

Basihyal excursions during raking power strokes in *Chitala* were then compared using linear regressions against the distance that the pectoral girdle was retracted and the amplitude of recruitment in the ventral TBA muscles (PIM, SH, and HP). An increased excursion of the basihyal during raking on goldfish was strongly positively correlated with an increase in pectoral girdle retraction (Frost and Sanford 1999; Fig. 8A) and with increased recruitment of the SH (Fig. 8B) and PIM (Fig. 8C), but strongly negatively correlated with recruitment of the HP (Fig. 8D). Only weak or very weak relationships existed between these variables for *Chitala* raking on worm. The relationship between modulation of pectoral girdle power stroke kinematics and contraction length dynamics in the PIM and SH in *Chitala* was finally examined graphically (Fig. 9). During raking power strokes on worm prey (Fig. 9A), the SH and PIM lengthen concomitantly with retraction of the pectoral girdle. However, during raking power strokes on fish prey (Fig. 9B), the PIM stores kinetic energy in an isotonic contraction lasting ~5–20 ms past the onset of pectoral girdle retraction. As pectoral girdle peak retraction is approached, the PIM then undergoes a rapid hyper-extension (ca. 200 mm s^{-1}).

Discussion

In both study taxa, we found congruent patterns between the presence and absence of modulation in TBA muscle activity and the previously quantified kinematic responses to evenly sized, but biomechanically contrasting prey-types during raking (Frost and Sanford 1999; Sanford 2001b). In the salmonid *Salvelinus*, neither muscle activity nor raking kinematics was modulated in response to differences in prey type. Therefore, this generalist predator does

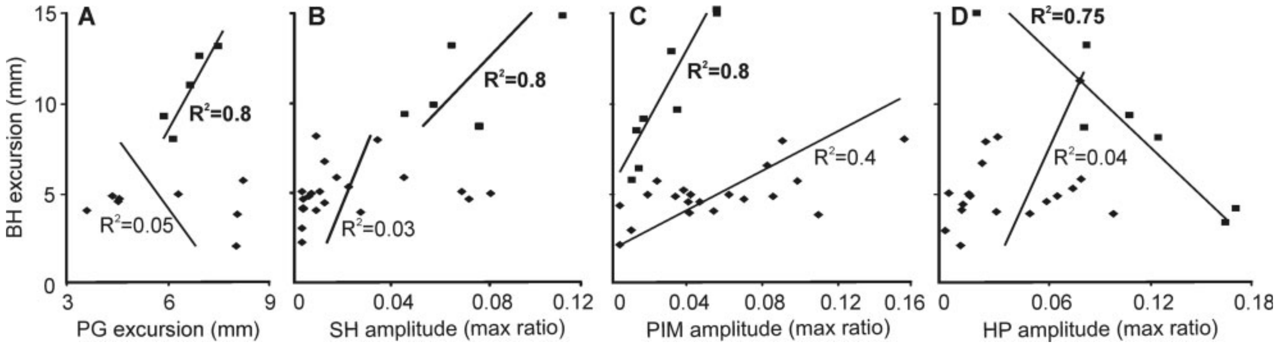

Fig. 8 Linear regressions of maximum excursion of the basihyal during raking power strokes in *Chitala*, measured using sonomicrometry during rakes on goldfish (squares) and on worms (diamonds), plotted against (**A**) magnitude of pectoral girdle retraction, measured from synchronized high-speed videos; and mean amplitudes of muscle activity of (**B**) the sternohyoid; (**C**) basihyal protractor and (**D**) hypaxial musculature, quantified using synchronized EMGs. High R^2-values show that the independent variables control basihyal excursion during raking on goldfish more rigorously than during raking on worms.

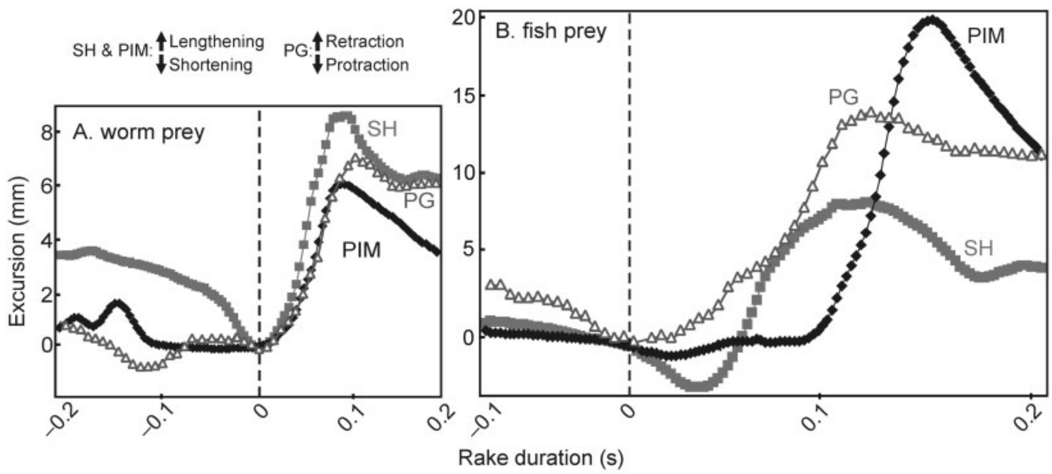

Fig. 9 Representative performance of *Chitala* raking on biomechanically contrasting **(A)** worm and (**B**) fish prey. Retraction of the pectoral girdle during the raking power stroke (PG, open grey triangles) was measured using motion analysis of high-speed videos and is indicated by an increase in excursion (*y*-axis). Length dynamics of the basihyal retractor (SH, grey squares) and protractors (PIM, black diamonds) were quantified using synchronized sonomicrometry. All variables were set to zero at the onset of neurocranial elevation (see Frost and Sanford 1999). Note that the SH is stretched ca. 8 mm during rakes on both prey types, which may cause reorientation, rather than a stretching of the CBL. That simultaneous shortening of the SH and retraction of the PG does lengthen the PIM early in the rake and may, given the difference in magnitude (2 mm) be caused by stretching of the integument at the surgical attachment of sonomicrometric crystals.

not conform to Liem's (1978, 1979) theorem, which predicts that trophic generalists stand to gain a greater increase in fitness by modulating a behavior than trophic specialists. In contrast, the osteoglossomorph *Chitala* modulated raking at both organizational levels, with an unexpected modulation of MAP involving elastic recoil in the retraction of the basihyal. During the raking power strokes of *Chitala* on goldfish prey, an earlier onset of activity in the basihyal retractor musculature, coupled with increased recruitment of the hyoid protractor, yielded energy storage in the hyoid protractor muscle. Evidence of elastic recoil or other derived mechanisms was neither found during *Chitala* rakes on worm prey, nor in *Salvelinus* rakes on either prey type. Despite the structural, mechanical, functional, and ecological contrasts in their feeding biology, *Salvelinus* and *Chitala* exhibit a virtually identical caudally-directed shearing basihyal power stroke on similar prey. This raking basihyal kinesis contrasts with the dorsoventrally directed trajectory during open-mouth chewing, as previously hypothesized (Sanford and Lauder 1989; Sanford 2001b).

Absence of Modulation in *Salvelinus*

Our first hypothesis, that *Salvelinus* modulates its raking MAP, was rejected, and this is the only taxon so far shown to possess a feeding MAP that remains entirely unmodulated across prey types in spite of being a trophic generalist (Wainwright and Friel 2001; Wainwright 2002). These results corroborate earlier evidence that *Salvelinus* does not modulate strike or prey-processing kinematics across three biomechanically contrasting prey-types, a kinematic scenario that possibly extends across the Salmoniformes (Sanford 2001b; Konow, unpublished data). A stereotypical raking MAP also exists in rainbow trout (*Oncorhynchus mykiss*) (Konow and Sanford 2008), and raking in salmonids in general may lack conformity with the "modulatory multiplicity" theorem of Liem (1978, 1979).

Both TBA morphology and biomechanics offer several corroborating lines of evidence as to why modulation may be lacking in the trophic generalists *Salvelinus* and its salmonid sister taxa. Firstly, the CBL in salmonids is arc-shaped, a qualitative trait that may place major anatomical constraints on TBA function and have given rise to the evolution of the conservative cranial anatomy among salmonids (Lauder and Liem 1980; Sanford 2000). Functionally, this CBL anatomy may be a trade-off that facilitates eccentric SH contraction, a common muscle behavior in suction feeders (van Wassenbergh et al. 2005, 2007). Extensive neurocranial kinesis during raking in *Salvelinus* (Sanford 2001b) may therefore be compensatory excursion in order to straighten the CBL and enable it to transmit hypaxial power to the basihyal. The larger anatomical cross-sectional area of the EP and HP, a known proxy for muscle power production (Carroll 2004), as well as a significantly smaller SH mass in *Salvelinus* compared to *Chitala* (A. L. Camp, N. Konow, and C. P. J. Sanford, unpublished data) also suggest that body musculature provides the primary input to the power stroke of raking in *Salvelinus*.

As a corollary, the raking power stroke in *Salvelinus* is driven by neurocranial elevation, which, aided by occlusion of the oral jaws and protraction of the basihyal, serves to displace the dentition of the upper TBA jaw (vomerine, parasphenoid) anteriorly relative to the dentition of the basihyal. Neurocranial elevation can be modeled as a third-order lever mechanism in which distances of the in-lever (epaxial distance) and out-lever (from the neurocranial articulation with the vertebral column to the anterior-most vomerine tooth) govern a trade-off between force and velocity (Carroll 2004). During raking in *Salvelinus*, the significantly elongated out-lever distance theoretically sacrifices efficient transmission of force for increased velocity of upper TBA jaw protraction (A. L. Camp, N. Konow, and C. P. J. Sanford, unpublished data). However, when viewed together with the relatively enlarged epaxial muscle architecture, it appears that *Salvelinus* may have sufficient muscle power to achieve high velocity movements while still maintaining the force-production necessary to successfully process any type of naturally encountered prey. Thus, TBA morphology and biomechanics, and raking muscle activity and kinematics in *Salvelinus* may result in a functionally unique system that relies on muscular and behavioral "brawn". This TBA may be biomechanically capable of a power stroke during raking that is both rapid and powerful, a rare trait in fish feeding (Anderson and Westneat 2007), which perhaps eliminates the need to modulate (Sanford 2001b).

Modulation in *Chitala*

Our second hypothesis, that modulation occurred in the raking MAPs of *Chitala*, was accepted, as MAP modulation was elicited by prey-type differences, as predicted by existing raking kinematics data (Frost and Sanford 1999). However, this result does not precisely conform to Liem's predictions (1978, 1979) either, since *Chitala* is a trophic specialist feeding on large and elusive benthopelagic prey (Rahman 1989; Lim et al. 1999). More importantly, most predictions about modulation of muscle activity arising from Frost and Sanford's (1999) study were not supported by our current results from EMG and sonomicrometry. The hyoid protractor (PIM) was recruited more during raking on biomechanically challenging prey than on non-elusive, malleable prey. As predicted, hypaxial activity was modulated, but surprisingly with an earlier onset of activity, and reduced amplitude during raking on goldfish (Fig. 5A). The increased mean duration of hypaxial activity during rakes on goldfish (88 versus 60 ms: Fig. 3) was statistically attributable to individual variability, and therefore did not explain the increased retraction of the pectoral girdle as predicted previously by Frost and Sanford (1999).

The relationship between the architecture and modulation of the hyoid protractor in *Chitala* is interesting because of the specialized myology, involving a significantly smaller anatomical cross-sectional area than in the functionally equivalent musculature in *Salvelinus*. The PIM in *Chitala* runs parallel with the mandible (Sanford and Lauder 1989), due to a shift in insertion from a transverse span of the proximal mandibular rami seen in basal teleosts ranging from *Amia* to the Salmoniformes (Greenwood 1971). The PIM in *Chitala* is therefore functionally homologous with the PH in euteleosts (Winterbottom 1974), which among osteoglossomorphs, both in more basal (*Hiodon*) and derived taxa (the Osteoglossidae), is formed by fusion of the PIM and interhyoideus muscles (Greenwood 1971; see also Hilton 2001). Functional implications of this specialized myology include significant elongation of this hyoid protractor (Sanford and Lauder 1990), and an associated increase in the length of its muscle fibers. As the potential for isotonic contraction in skeletal muscle scales positively with fiber length (Carroll 2004), the PIM in *Chitala* being longer than its functional equivalent in *Salvelinus* (PH) could undergo greater shortening. We quantified excursions of the basihyal from maximally protracted to maximally retracted during raking power strokes on goldfish in both taxa that approached 25 mm, or 40% HL, which closely matches manipulation estimates in Sanford and Lauder (1989) (Figs 6 and 7). This interesting example of how biomechanics can cause strongly convergent kinematic output to result from divergent inputs thus at least indirectly corroborates previous assumptions that different power stroke mechanisms could be powering similar raking behaviors in these study taxa.

Overlap of MAP phases in *Chitala*

The prey-type effect in the raking MAP of *Chitala* involved a distinct overlap in activity of the mandible adductor and hyoid protractor muscles driving the raking preparatory phase, and the HP, EP, and SH muscles driving the power-stroke. This appears to be a trend in the osteoglossomorph raking MAP that is not matched among salmonids. In the arowana (*Scleropages jardinii*), such an overlap was also evident but it was only quantified for the elusive and robust prey type (goldfish; Konow and Sanford 2008). The pattern in *Chitala* may be a variation on the osteoglossomorph theme, as not only does the activity of the preparatory musculature extend past the onset of the power stroke (as indicated by onset of epaxial activity; Fig. 3) like in *Scleropages*, but hypaxial and SH muscle activity also commence well before the onset of the raking power stroke during rakes on goldfish.

The inclusion of temporal shifts in muscle activity in the principal traits driving modulation of the raking MAP in *Chitala* is an unusual finding given that duration of muscle activity is generally considered to be under tight neuromotor control by central pattern generators (Ross et al. 2007; Herrel et al. 2008). Motor-pattern research has until now discovered that such activity-changes (onset-timing and duration of activity) generally result from evolutionary shifts in musculoskeletal function, while recruitment variables (amplitude and integrated area) are more labile and thus more likely to facilitate behavioral changes (Alfaro et al. 2001; Alfaro and Herrel 2001; Wainwright and Friel 2001; Wainwright 2002; Konow and Sanford 2008).

The temporal shifts in MAP presented here result in more prolonged overlap in the activity of antagonistic muscle groups in the ventral TBA of *Chitala* than in *Scleropages* (Konow and Sanford 2008), with clear functional consequences. In addition to facilitating elastic recoiling of the basihyal, this overlap between the activity of preparatory and power stroke muscles may also augment occlusion of the oral jaws, resulting in further compression, and thus more efficient reduction and/or immobilization of the prey (Konow and Sanford 2008). Already a well-documented mechanism in the biomechanics of vertebrate feeding (Aerts et al. 1987; Konow and Bellwood 2005; Lappin et al. 2006; Van Wassenbergh et al. 2008), energy-storage, and subsequent elastic recoil adequately explain the otherwise counter-intuitive relationship between an increase in basihyal excursion and reduced recruitment of the hypaxial muscles during rakes on goldfish. It is noteworthy that Van Wassenbergh et al. (2008) observed: "the energy-storing structure in elastic recoil mechanisms need not have a higher power potential than the effector structure" (van Wassenbergh et al. 2008), these being the gracile PIM and massive SH muscles, respectively, in *Chitala*.

The SH-CBL complex

The CBL directly connects the pectoral girdle to the basihyal and may be a key structural innovation that facilitates elastic recoil during raking on biomechanically challenging prey in *Chitala*. Motion produced by retraction of the pectoral girdle is possibly more directly transmitted to basihyal motion in *Chitala* via the prominent, short, and straight CBL, than in *Salvelinus* (see above). Additionally, a suite of highly specialized post-cranial morphological traits in *Chitala* could help in facilitating recruitment of the caudal HP for retraction of the basihyal during raking on particularly robust prey. These structures include the discontinuous pleural ribs, a hypertrophied and hinged anal pterygiophore, and a row of ventral scutes between this pterygiophore and the pectoral girdle (Hilton 2003). The hinge of the pectoral girdle is dorsally displaced in *Chitala*, by a significantly smaller supracleithrum than in *Salvelinus* (Lauder and Liem 1980; Hilton 2003). A unique aspect of the TBA in *Chitala* and notopterids in general, relative to all other TBA-bearing fishes, is the presence of an autogenous bony element associated with the second basibranchial (Taverne 1978; Sanford and Lauder 1989; Hilton 2003) upon which the CBL and at least some fibers of the SH insert. By providing an alternative insertion site for both the CBL and the SH, this novel bony element represents an additional degree of freedom in the ventral complex of the TBA that could be involved in the observed modulation. Together, these divergent morphological traits may also explain the emphasis on pectoral girdle kinematics during raking in *Chitala* (Sanford and Lauder 1989; Frost and Sanford 1999). Experiments are currently underway to examine the functional role of the CBL by severing it at the superficial attachment onto the medial face of the proximal autogenous process, testing a prediction that the CBL permits functional decoupling in the TBA. Evidence of discontinued modulation, including omission of elastic recoil during raking on goldfish, or a more stereotypical MAP in any raking muscle after severance of the CBL would empirically prove the hypothesis of functional decoupling.

We found an unmodulated, low-intensity and highly variable recruitment of the SH during raking in *Chitala* contrasting with an earlier study of notopterid MAPs, in which activity of the SH was altogether lacking in >33% of rakes (Sanford and Lauder 1990). We only detected silence in the SH in one of five individuals and then only in ca. 2% of the rakes recorded. This discrepancy could be explained by improvements in equipment and protocol over the past decades or by individual variation. The present MAP evidence corresponds well with a significantly more massive SH in *Chitala* than in *Salvelinus* (A. L. Camp, N. Konow, and C. P. J. Sanford, unpublished data). However, the present results do not reject the hypothesis by Sanford and Lauder (1989) that modulation of SH activity would be important evidence of structural duplication of this muscle by the CBL and thus decoupling of the SH to act as a modulator. Firstly, relegation of SH variables to the second canonical correspondence axis in the DFA may be due to the overriding statistical effect of the early onset and extended duration in preparatory muscle activity, known to be a convergently derived MAP giverning osteoglossomorph and salmonid raking (Konow and Sanford 2008). Secondly, the lack of detectable modulation of the SH does not preclude that the CBL may functionally decouple other muscles or that the SH, given the present elastic recoil evidence, functions differently than predicted by Sanford and Lauder (1989). Thirdly, the low and highly variable recruitment of the SH (see also Alfaro et al. 2001; Carroll 2004) severely weakens our ability to statistically establish quantitative differences in the MAP of this muscle. Therefore, the hypothesis of functional decoupling is preliminarily supported on the grounds of behavioral modulation being present at the organizational levels of muscle activity and kinematics in *Chitala*. The functionally and/or behaviorally mediated stereotypy in *Salvelinus* does not offer convincing grounds for rejecting the decoupling hypothesis, as lack of modulation may be caused by structural trade-off's between raking and more ancestral behaviors.

Conclusions

Despite the convergent evolution of prominent fang-like basihyal dentition, we hypothesized that trajectories of the basihyal in the study taxa would diverge due to previously quantified differences in raking kinematics (see Sanford and Lauder 1989; Frost and Sanford 1999; Sanford 2001b), and in the morphology and biomechanics of the TBA. Although we discovered that raking MAPs, in common with overall kinematics, differ between taxa, we also unexpectedly detected a strong convergence in the kinesis of the basihyal during rakes. Therefore, the TBA muscle activity and raking kinematics in the osteoglossomorph and salmonid representatives studied here provides an important and novel biological example of convergent function in spite of divergence in the musculoskeletal mechanisms powering the system.

Acknowledgments

We thank M. Kats for help with experiments, the Hofstra University Animal Care Facility staff for specimen care, Long Island Aquatics and Cold Spring Harbor Fish Hatchery for specimens, and P. Doherty for comments on early drafts. One author (N.K.) thanks the Society for Integrative and Comparative Biology, the Division of Comparative Biomechanics, the Journal of Experimental Biology, ADInstruments and Grass electronics for their financial support of the late-breaking symposium on *Electromyography: Interpretation and Limitations in Functional Analyses of Musculoskeletal Systems* at the 2008 annual SICB meeting. Work presented herein was supported by the National Science Foundation (IOS#0444891, DBI#420440) to CPJS.

References

Aerts P, De Vree F. 1993. Feeding performance and muscular constraints in fish. J Exp Biol 177:129–47.

Aerts P, Osse JWM, Verraes W. 1987. A model of jaw depression during feeding in *Astatotilapia elegans* (Teleostei: Cichlidae): mechanisms for energy storage and triggering. J Morph 194:85–109.

Ajemian MJ, Sanford CP. 2007. Food capture kinematics in the deep-water chain catshark *Scyliorhinus retifer*. J Mar Biol Ass UK 87:1277–86.

Alfaro ME, Herrel A. 2001. Introduction: major issues of feeding motor control in vertebrates. Am Zool 41:1243–7.

Alfaro ME, Janowetz J, Westneat MW. 2001. Motor control across trophic strategies: muscle activity of biting and suction feeding fishes. Am Zool 41:1266–79.

Alfaro ME, Westneat MW. 1999. Motor patterns of herbivorous feeding: electromyographic analysis of biting in the parrotfishes *Cetoscarus bicolor* and *Scarus iseri*. Brain Behav Evol 54:205–22.

Anderson CW. 1993. The modulation of feeding behaviour in response to prey type in the frog *Rana pipiens*. J Exp Biol 179:1–12.

Anderson PSL, Westneat MW. 2007. Feeding mechanics and bite force modelling of the skull of *Dunkleosteus terrelli*, an ancient apex predator. Biol Lett 3:76–9.

Bolnick DI, Ferry-Graham LA. 2002. Optimizing prey-capture behaviour to maximize expected net benefit. Evol Ecol Res 4:843–55.

Carroll AM. 2004. Muscle activation and strain during suction feeding in the largemouth bass, *Micropterus salmoides*. J Exp Biol 207:983–91.

Deban SM, O'Reilly JC, Nishikawa KC. 2001. The evolution of the motor control of feeding in amphibians. Am Zool 41:1280–98.

Ferry-Graham LA. 1998. Effects of prey size and mobility on prey-capture kinematics in leopard sharks *Triakis semifasciata*. J Exp Biol 201:2433–44.

Ferry-Graham LA, Wainwright PC, Westneat MW, Bellwood DR. 2001. Modulation of prey capture kinematics in the cheeklined wrasse *Oxycheilinus digrammus* (Teleostei: Labridae). J Exp Zool 290:88–100.

Frost BJ, Sanford CPJ. 1999. Kinematics of a novel feeding mechanism in the osteoglossomorph fish *Chitala chitala*: is there a prey-type effect? Zoology 102:18–30.

Galis F. 1993. Interactions between the pharyngeal jaw apparatus, feeding behaviour, and ontogeny in the cichlid fish, *Haplochromis piceatus*: a study of morphological constraints in evolutionary ecology. J Exp Zool 267:137–54.

Greenwood PH. 1971. Hyoid and ventral gill arch musculature in osteoglossomorph fishes. Bull Br Mus Nat Hist Zool 22:1–55.

Grubich JR. 2001. Prey capture in actinopterygian fishes: a review of suction feeding motor patterns with new evidence from an elopomorph fish, *Megalops atlanticus*. Am Zool 41:1258–65.

Herrel A, Schaerlaeken V, Ross CF, Meyers J, Nishikawa K, Abdala V, Manzano A, Aerts P. 2008. Electromyography and the evolution of motor control: limitations and insights. Integr Comp Biol. doi: 10.1093/icb/icn025.

Hilton EJ. 2001. Tongue bite apparatus of osteoglossomorph fishes: variation of a character complex. Copeia 2001:372–81.

Hilton EJ. 2003. Comparative osteology and phylognetic systematics of fossil and living bony-tongue fishes (Actinopterygii, Teleostei; Osteoglossomorpha). Zool J Linn Soc 137:1–100.

Konow N, Bellwood DR. 2005. Prey-capture in *Pomacanthus semicirculatus* (Teleostei, Pomacanthidae): functional implications of intramandibular joints in marine angelfishes. J Exp Biol 208:1421–33.

Konow N, Sanford CPJ. 2008. Is a convergently derived muscle-activity pattern driving novel raking behaviours in teleost fishes? J Exp Biol 211:989–99.

Korff WL, Wainwright PC. 2004. Motor pattern control for increasing crushing force in the striped burrfish (*Chilomycterus schoepfi*). Zoology 107:335–46.

Lappin AK, Monroy JA, Pilarski JQ, Zepnewski ED, Pierotti DJ, Nishikawa KC. 2006. Storage and recovery of elastic potential energy powers ballistic prey capture in toads. J Exp Biol 209:2535–53.

Lauder GV, Liem KF. 1980. The feeding mechanism and cephalic myology of *Salvelinus fontinalis*: Form, function, and evolutionary significance. In: Balon EK, editor. Charrs: Salomnids of the genus Salvelinus. Netherlands: Junk Publishers. p. 365–90.

Lauder GV, Prendergast T. 1992. Kinematics of aquatic prey capture in the snapping turtle, *Chelydra serpentina*. J Exp Biol 164:55–78.

Lauder GV, Reilly SM. 1996. The mechanistic bases of behavioural evolution: a multivariate analysis of musculoskeletal function. In: Martins E, editor. Phylogenies and the comparative method in animal behavior. Cambridge: Oxford University Press. p. 104–37.

Liem KF. 1978. Modulatory multiplicity in the functional repertoire of the feeding mechanism in cichlid fishes. I Piscivores J Morphol 158:323–60.

Liem KF. 1979. Adaptive significance of intra- and interspecific differences in the feeding repertoires of cichlid fishes. Am Zool 20:295–314.

Lim P, Lek S, Touch ST, Mao S-O, Chhouk B. 1999. Diversity and spatial distribution of freshwater fish in Great Lake and Tonle Sap River (Cambodia, Southeast Asia). Aquat Living Resour 12:379–86.

Motta PJ, Wilga CD. 2001. Advances in the study of feeding behaviors, mechanisms, and mechanics of sharks. Env Biol Fish 60:131–56.

Munday PL, Wilson SK. 1997. Comparative efficacy of clove oil and other chemicals in anaesthetization of *Pomacentrus amboinensis*, a coral reef fish. J Fish Biol 51:931–8.

Nemeth DH. 1997a. Modulation of buccal pressure during prey capture in *Hexagrammos decagrammus* (Teleostei: Hexagrammidae). J Exp Biol 200:2145–54.

Nemeth DH. 1997b. Modulation of attack behavior and its effect on feeding performance in a trophic generalist fish, Hexagrammos decagrammus. J Exp Biol 200:2155–64.

Ojanguren AF, Brana F. 2000. Thermal dependence of swimming endurance in juvenile brown trout. J Fish Biol 56:1342–7.

Rahman AKA. 1989. Freshwater fishes of Bangladesh. Zoological Society of Bangladesh. Dhaka: Department of Zoology, University of Dhaka. p. 364.

Ralston KR, Wainwright PC. 1997. Functional consequences of trophic specialization in pufferfishes. Funct Ecol 11:43–52.

Reilly SM, Lauder GV. 1989. Physiological bases of feeding behaviour in salamanders: do motor patterns vary with prey type? J *Exp Biol* 141:343–58.

Ross CF, Eckhardt A, Herrel A, Hylander WL, Metzger KA, Schaerlaeken V, Washington RL, Williams SH. 2007. Modulation of intra-oral processing in mammals and lepidosaurs. Integr Comp Biol 47:118–36.

Roth G, Wake DB. 1985. Trends in the functional morphology and sensorimotor control of feeding behavior in salamanders: an example of the role of internal dynamics in evolution. Acta Biotheor 34:175–91.

Sanford CPJ. 2000. Salmonoid fish osteology and phylogeny (Teleostei, Salmonoidei). Ruggell/Liechtenstein: A.R.G. Gantner Verlag KG.

Sanford CPJ. 2001a. The novel 'tongue-bite apparatus' in the knifefish family Notopteridae (Teleostei: Osteoglossomorpha): are kinematic patterns conserved within a clade? Zool J Linn Soc 132:259–75.

Sanford CPJ. 2001b. Kinematic analysis of a novel feeding mechanism in the brook trout Salvelinus fontinalis (Teleostei: Salmonidae): behavioural modulation of a functional novelty. J Exp Biol 204:3905–16.

Sanford CPJ, Lauder GV. 1989. Functional morphology of the "Tongue-Bite" in the Osteoglossomorph fish *Notopterus*. J Morph 202:379–408.

Sanford CPJ, Lauder GV. 1990. kinematics of the tongue-bite apparatus in osteoglossomorph fishes. J Exp Biol 154:137–62.

Sanford CPJ, Wainwright PC. 2002. Use of sonomicrometry demonstrates the link between prey capture kinematics and suction pressure in largemouth bass. J Exp Biol 205:3445–57.

Streelman JT, Danley PD. 2003. The stages of vertebrate evolutionary radiation. Trends Ecol Evol 118:126–31.

Taverne L. 1978. Ostéologie, phylogénése et systématique des Téléostéens fossiles et actuels du super-ordre des Ostéoglossomorphes. Deuxiéme partie. Ostéologie des genres *Phaerodus*, *Phareoides*, *Brychaetus*, *Musperia*, *Pantodon*, *Singida*, *Notopterus*, *Xenomystus* et *Papyrocranus*. Académie Royale de Belgique, Mémoirs de la Classe des Sciences, Collection in-84, 2e. série 42: 1–212.

Van Wassenbergh S, Herrel A, Adriaens D, Aerts P. 2005. A test of mouth-opening and hyoid-depression mechanisms during prey capture in a catfish. J Exp Biol 208:4627–39.

Van Wassenbergh S, Herrel A, Adriaens D, Aerts P. 2006. Modulation and variability of prey capture kinematics in clariid catfishes. J Exp Zool 305A:559–69.

Van Wassenbergh S, Herrel A, Adriaens D, Aerts P. 2007. Interspecific variation in sternohyoideus muscle morphology in clariid catfishes: functional implications for suction feeding. J Morphol 268:232–42.

Van Wassenbergh S, Strother JA, Flammang BE, Ferry-Graham LA, Aerts P. 2008. Extremely fast prey capture in pipefish is powered by elastic recoil. J R Soc Interface 5:285–96.

Wainwright PC. 1986. Motor correlates of learning behaviour: feeding on novel prey by pumpkinseed sunfish (*Lepomis gibbosus*). J Exp Biol 126:237–47.

Wainwright PC. 2002. The evolution of feeding motor patterns in vertebrates. Curr Opin Neurobiol 12:691–5.

Wainwright PC, Friel JP. 2000. Effects of prey type on motor pattern variance in tetraodontiform fishes. J Exp Zool 286:563–71.

Wainwright PC, Friel JP. 2001. Behavioral characters and historical properties of motor patterns. In: Wagner G, editor. The character concept in evolutionary biology. San Diego: Academic Press. p. 285–301.

Wainwright PC, Lauder GV. 1986. Feeding biology of sunfishes: patterns of variation in the feeding mechanism. Zool J Linn Soc 88:217–28.

Wainwright PC, Richard BA. 1995. Scaling the feeding mechanism of the largemouth bass (*Micropterus salmoides*): motor patterns. J Exp Biol 198:1161–71.

Wainwright PC, Sanford CP, Reilly SM, Lauder GV. 1989. Evolution of motor patterns: aquatic feeding in salamanders and ray-finned fishes. Brain Behav Evol 34:324–41.

Wilga CD, Motta PJ. 1998. Feeding mechanism of the Atlantic guitarfish *Rhinobatus lentiginosus*: modulation of kinematic and motor activity? J Exp Biol 201:3167–83.

Winterbottom R. 1974. A descriptive synonymy of the striated muscles of the Teleostei. Proc Acad Nat Sci Philad 125:225–317.

Zar JH. 1999. Biostatistical analysis. 4th Edition. New Jersey: Prentice Hall. p. 663.